JOURNAL OF THE AMERICAN COLLEGE OF CARDIOLOGY VOL. 72, NO. 9, 2018
© 2018 BY THE AMERICAN COLLEGE OF CARDIOLOGY FOUNDATION
PUBLISHED BY ELSEVIER

Myocardial Infarction Produces Sustained Proinflammatory Endothelial Activation in Remote Arteries

Federico Moccetti, MD,[a] Eran Brown, MS,[a] Aris Xie, MS,[a] William Packwood, BS,[a] Yue Qi, MD,[a] Zaverio Ruggeri, PhD,[b] Weihui Shentu, MD,[a] Junmei Chen, PhD,[c] Jose A. López, MD,[c] Jonathan R. Lindner, MD[a,d]

ABSTRACT

BACKGROUND In the months after acute myocardial infarction (MI), risk for acute atherothrombotic events in nonculprit arteries increases several fold.

OBJECTIVES This study investigated whether sustained proinflammatory and prothrombotic endothelial alterations occur in remote vessels after MI.

METHODS Wild-type mice, atherosclerotic mice with double knockout (DKO) of the low-density lipoprotein receptor and Apobec-1, and DKO mice treated with the Nox-inhibitor apocynin were studied at baseline and at 3 and 21 days after closed-chest MI. Ultrasound molecular imaging of P-selectin, vascular cell adhesion molecule (VCAM)-1, von Willebrand factor (VWF) A1-domain, and platelet GPIbα was performed. Intravital microscopy was used to characterize post-MI leukocyte and platelet recruitment in the remote microcirculation after MI.

RESULTS Aortic molecular imaging for P-selectin, VCAM-1, VWF-A1, and platelets was increased several-fold ($p < 0.01$) 3 days post-MI for both wild-type and DKO mice. At 21 days, these changes resolved in wild-type mice but persisted in DKO mice. Signal for platelet adhesion was abolished 1 h after administration of ADAMTS13, which regulates VWF multimerization. In DKO and wild-type mice, apocynin significantly attenuated the post-MI increase for molecular targets, and platelet depletion significantly reduced P-selectin and VCAM-1 signal. On intravital microscopy, MI resulted in remote vessel leukocyte adhesion and platelet string or net complexes. On histology, high-risk inflammatory features in aortic plaque increased in DKO mice 21 days post-MI, which were completely prevented by apocynin.

CONCLUSIONS Acute MI stimulates a spectrum of changes in remote vessels, including up-regulation of endothelial inflammatory adhesion molecules and platelet-endothelial adhesion from endothelial-associated VWF multimers. These remote arterial alterations persist longer in the presence of hyperlipidemia, are associated with accelerated plaque growth and inflammation, and are attenuated by Nox inhibition. (J Am Coll Cardiol 2018;72:1015–26)
© 2018 by the American College of Cardiology Foundation.

Major acute atherothrombotic events such as myocardial infarction (MI), stroke, or limb ischemia lead to a markedly increased risk for recurrent events in separate vascular territories. After MI, the risk for stroke or recurrent MI from nonculprit lesions is increased by several-fold over the ensuing 6 to 12 months (1–3). These findings indicate that a focal ischemic event can lead to systemic adverse vascular responses. Murine studies have demonstrated that acute MI triggers the splenic

Listen to this manuscript's audio summary by *JACC* Editor-in-Chief Dr. Valentin Fuster.

From the [a]Knight Cardiovascular Institute, Oregon Health & Science University, Portland, Oregon; [b]Department of Molecular and Experimental Medicine, Scripps Research Institute, La Jolla, California; [c]Bloodworks NW, Seattle, Washington; and the [d]Oregon National Primate Research Center, Oregon Health & Science University, Portland, Oregon. Dr. Moccetti has received support from a grant from the Swiss National Science Foundation. Dr. Ruggeri has received support from National Institutes of Health (NIH) grants HL42846 and HL78784. Dr. López has received support from NIH grants R01-HL091153 and R01-HL11763. Dr. Lindner has received support from NIH grants R01-HL078610, R01-HL130046, and P51-OD011092; and grant 14-14NSBRI1-0025 from the NASA National Space Biomedical Research Institute. All other authors have reported that they have no relationships relevant to the contents of this paper to disclose.

Manuscript received February 16, 2018; revised manuscript received June 7, 2018, accepted June 10, 2018.

ISSN 0735-1097/$36.00 https://doi.org/10.1016/j.jacc.2018.06.044

ABBREVIATIONS AND ACRONYMS

ADAMTS13 = A disintegrin and metalloprotease with thrombospondin type I repeats-13

CEU = contrast-enhanced ultrasound

DKO = double knockout

VCAM = vascular cell adhesion molecule

VWF = von Willebrand factor

production and mobilization of inflammatory Ly-6C^{high} monocytes, and the accelerated entry of these cells and other CD11b+ myeloid cells into remote arterial plaque for weeks after the initial event (4). With regard to remote vascular endothelial responses, MI in mice leads to up-regulation of mRNA for endothelial cell adhesion molecules within the noninfarct myocardial microcirculation (5). However, little is known about endothelial-specific alterations in remote arterial atherosclerotic lesions, including in noncoronary locations.

SEE PAGE 1027

In this study, in vivo imaging methods, unique in their ability to investigate events at the endothelial-blood pool interface, were used to study post-MI endothelial alterations in remote arteries that can predispose to accelerated plaque growth and atherothrombotic events. Contrast-enhanced ultrasound (CEU) molecular imaging and direct microvascular observation with intravital microscopy were used to characterize the endothelial responses that occur in remote arteries after MI. CEU molecular imaging with targeted microbubble contrast agents that are confined to the vascular compartment was selected based on extensive experience in murine and nonhuman primate models to detect arterial events that occur at the endothelial-blood pool interface (6–8). Specifically, we hypothesized that acute MI leads to: 1) remote arterial up-regulation of endothelial cell adhesion molecules on the plaque surface; and 2) platelet adhesion to the intact endothelial surface, which contributes to proinflammatory activation and can occur, in part, from abnormal, endothelial-associated, ultra-large, self-associated multimers of von Willebrand factor (VWF) that occur secondary to dysregulation of normal proteolytic regulation by ADAMTS13 (a disintegrin and metalloprotease with thrombospondin type I repeats-13) (9–11).

METHODS

ANIMAL MODEL. The study was approved by the Animal Care and Use Committee of the Oregon Health & Science University. We studied wild-type C57Bl/6 mice and mice with susceptibility to age-related atherosclerosis through dual gene-targeted deletion or "double knockout" (DKO) of the low-density lipoprotein receptor and apolipoprotein-B mRNA editing enzyme catalytic polypeptide 1 (Apobec-1) on a C57Bl/6 background. DKO mice develop reproducible, age-dependent development of atherosclerosis on a chow diet (6,12), and were studied at 20 to 25 weeks of age, when plaque size is modest with early intraluminal encroachment (6). For all studies, mice were anesthetized with 1.0% to 2.0% inhaled isoflurane, and a jugular cannula was placed for intravenous (IV) injection of contrast agents or drugs.

IMAGING STUDY DESIGN. The proximal thoracic aorta was selected as a remote arterial site to study endothelial activation after MI. CEU molecular imaging of the aorta was performed using microbubble contrast agents targeted to P-selectin (MB_P), vascular cell adhesion molecule (VCAM)-1 (MB_V), GPIbα as an indicator of platelet adhesion (MB_{Plt}), and endothelial VWF (MB_{VWF}). Studies were also performed with control nontargeted microbubbles (MB). Animals were studied in the following experimental conditions:

1. Molecular imaging was performed at baseline and at either 3 or 21 days after MI in wild-type and DKO mice. Mice were also studied 3 days after sham procedure.
2. Molecular imaging was performed 3 days after MI in DKO mice treated 1 h prior to imaging with recombinant human ADAMTS13 (5 μg IV), the key regulatory protease that reduces VWF multimer size through cleavage at the VWF A2 domain (10,11).
3. Molecular imaging was performed 3 and 21 days after MI in DKO mice treated with apocynin (50 mg/kg/day) starting on the day of MI. Apocynin (acetovanillone) is a potent inhibitor of NADPH-oxidase (Nox), which has been implicated in transcriptional up-regulation of adhesion molecule expression and has been demonstrated to reduce platelet-endothelial adhesion in early and late atherosclerosis (13,14).
4. Molecular imaging was performed 21 days after MI in DKO mice undergoing platelet depletion by IV injection of 2 μg/g rat antimouse GPIbα monoclonal antibody (7) at days 1, 4, 9, and 15 post-MI to determine the contribution of platelets to sustained endothelial adhesion molecule expression.

MYOCARDIAL INFARCTION. A closed-chest model of MI was used to allow for the resolution of the acute inflammatory responses after thoracotomy and cardiac exposure. At least 5 days prior to scheduled MI, mice were anesthetized, intubated, and placed on positive pressure mechanical ventilation with weight-adjusted tidal volumes and respiratory rates. A limited left lateral thoracotomy was performed to expose only the basal anterior wall. A 6-0 prolene suture was placed under the left anterior descending

FIGURE 1 Echocardiography and Vascular Ultrasound

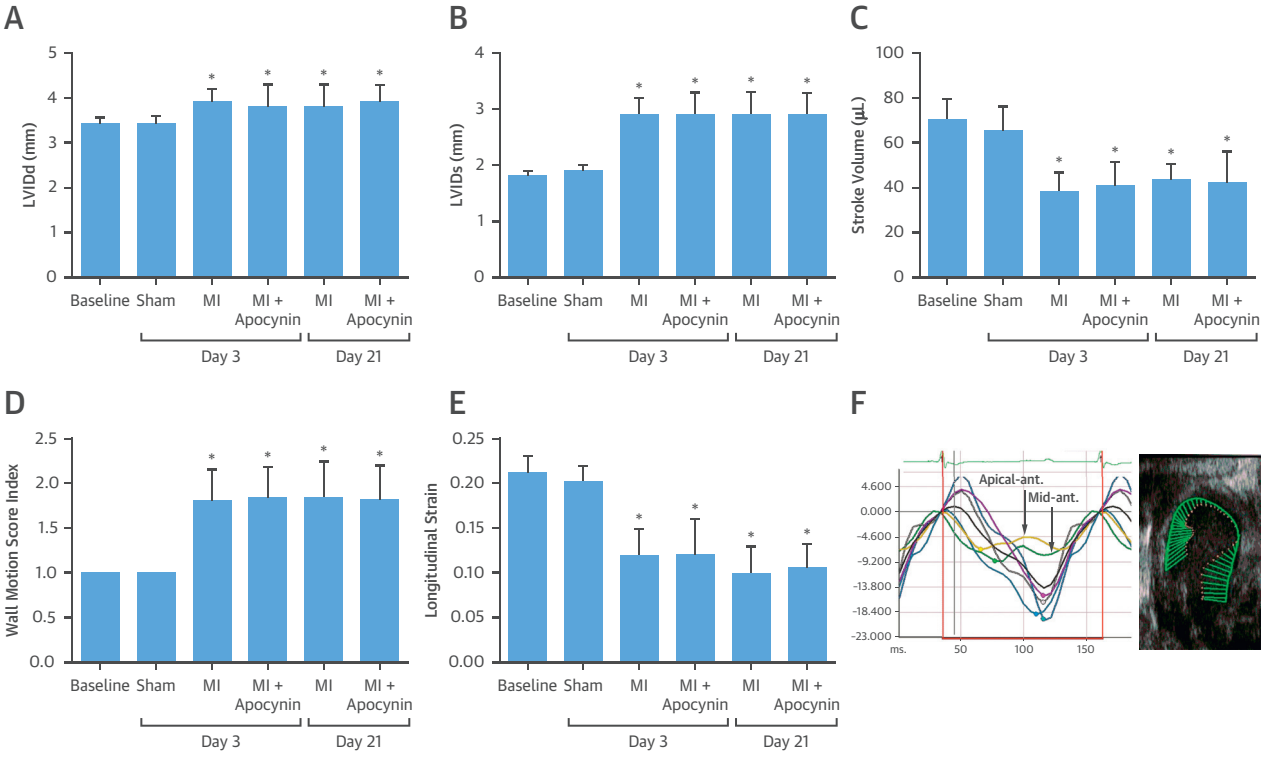

Mean ± SD values are shown for **(A)** left ventricular internal diameter at end-diastole (LVIDd), **(B)** left ventricular internal diameter at end-diastole end-systole (LVIDs), **(C)** stroke volume, **(D)** wall motion score index, and **(E)** longitudinal strain. Data are combined for wild-type and double knockout mice, which were not significantly different from each other. *$p < 0.05$ versus baseline. **(F)** Example of left ventricular strain curves from a long-axis view illustrating severe hypokinesis in the left anterior descending coronary artery territory at day 3 post-myocardial infarction (MI) and corresponding vector mapping of endocardial strain.

coronary artery but was left unsecured. The free ends of the suture were exteriorized through the chest wall and left in a subcutaneous location after closure. After 5 to 7 days, mice were anesthetized, the suture was exteriorized through a limited skin incision, and the tension was placed on the suture for 40 min to produce ST-segment elevation on electrocardiographic monitoring and wall motion abnormalities on high-frequency transthoracic 2-dimensional echocardiography (Vevo 2100, Visualsonics Inc., Toronto, Ontario, Canada). Sham-treated animals received a suture without tightening.

TARGETED MICROBUBBLE PREPARATION. Biotinylated lipid-shelled decafluorobutane microbubbles were prepared by sonication of a gas-saturated aqueous suspension of distearoylphosphatidylcholine (2 mg/ml), polyoxyethylene-40-stearate (1 mg/ml), and distearoylphosphatidylethanolamine-PEG(2000)biotin (0.4 mg/ml). Conjugation of biotinylated ligand to the microbubble surface was performed with biotin-streptavidin bridging as previously described (15). Ligands used for targeting were: dimeric murine recombinant A1 domain of VWF A1 (mature VWF amino acids 445 to 716) for targeting platelet GPIbα for MB_{Plt}, a cell-derived peptide representing the N-terminal 300 amino acids of GPIbα for MB_{VWF} (7), and monoclonal antibodies against the extracellular domain of either P-selectin (RB40.34, BD Biosciences, San Jose, California), or VCAM-1 (clone 429, BD Biosciences) for MB_P and MB_V, respectively. Control MB were prepared with isotype control antibody (R3-34, BD Biosciences). Microbubble concentrations and size distributions were measured by electrozone sensing (Multisizer III, Beckman Coulter, Brea, California).

IMAGING PROTOCOLS. CEU molecular imaging of the ascending aorta and proximal aortic arch was performed using a right parasternal window with a linear-array probe (Sequoia, Siemens Medical Systems, Mountain View, California). Multipulse phase-inversion and amplitude-modulation imaging at 7 MHz was performed with a dynamic range of 55 dB and a mechanical index of 1.0. Gain was set at a level

FIGURE 2 Molecular Imaging of Remote Endothelial Activation

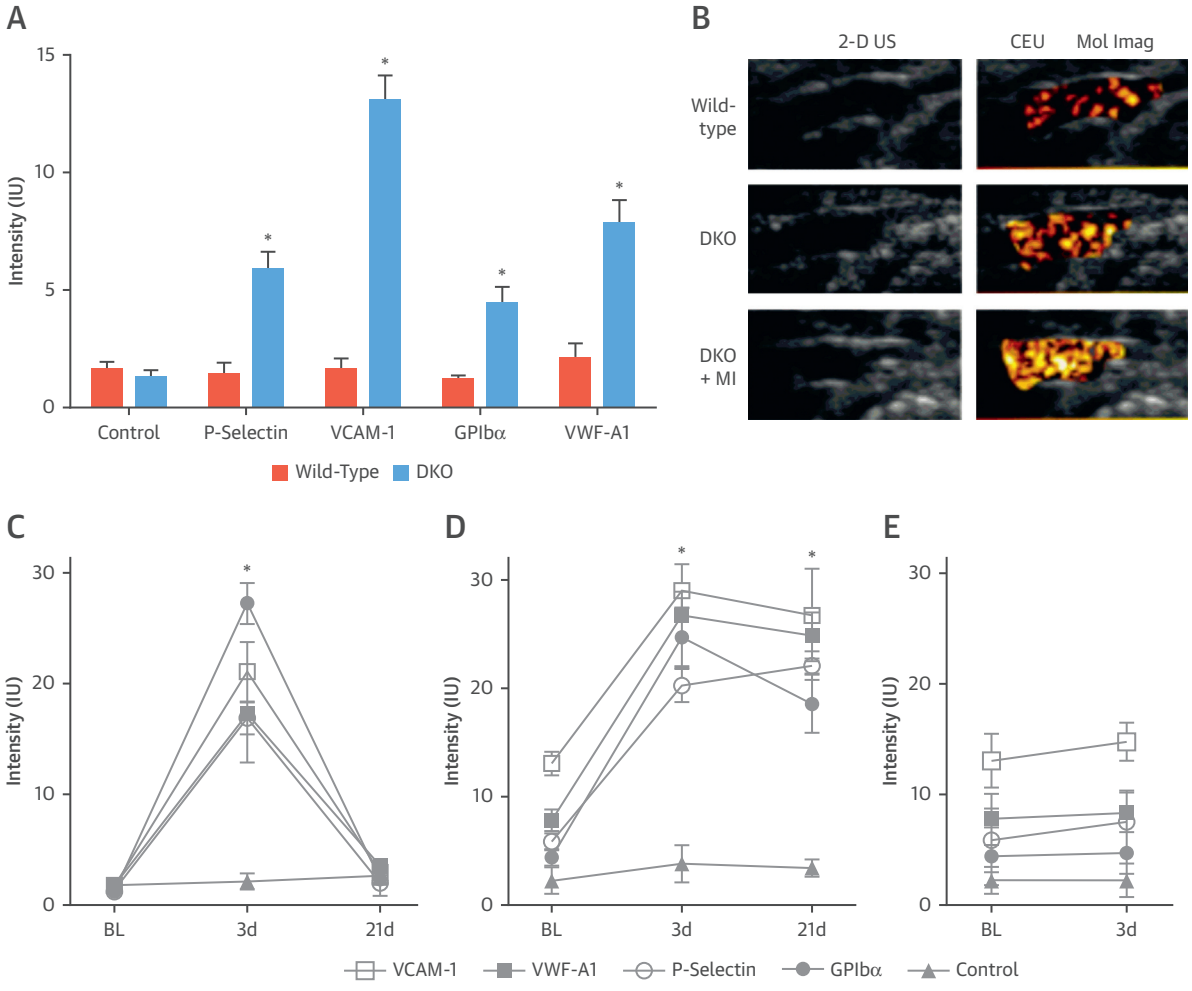

(A) Baseline (pre-myocardial infarction [MI]) background-subtracted signal intensity (mean ± SEM) on contrast-enhanced ultrasound (CEU) molecular imaging of the thoracic aorta from wild-type and double knockout (DKO) mice. *$p < 0.05$ versus control nontargeted signal. **(B)** Examples of 2-dimensional (2-D) ultrasound (US) and CEU molecular imaging for vascular cell adhesion molecule (VCAM)-1 of the thoracic aorta of wild-type, DKO, and post-MI (day 3) DKO mice. **(C to E)** Mean ± SEM signal intensity on CEU molecular imaging of the aorta from: **(C)** post-MI wild-type mice; **(D)** post-MI DKO mice; and **(E)** DKO mice undergoing sham surgery. *$p < 0.05$ for all actively-targeted agents versus baseline values and versus control nontargeted signal. BL = baseline; Mol Imag = molecular imaging; VWF = von Willebrand factor.

that just eliminated pre-contrast background speckle and kept constant for all studies. Images were acquired 8 min after intravenous injection of targeted or control microbubbles (1×10^6), performed in random order, to allow almost all free microbubbles to clear from blood pool. Signal from retained microbubbles alone was determined, as previously described, by acquiring the first ultrasound frame and then digitally subtracting several averaged frames obtained after complete destruction of microbubbles at a mechanical index of 1.4 to eliminate signal from the low concentration of freely-circulating microbubbles in the blood pool (15). Signal intensity was measured from a region-of-interest encompassing the entire ascending aorta to just beyond the origin of the brachiocephalic artery. Region selection was facilitated by fundamental 2-dimensional imaging at 14 MHz acquired after each CEU imaging sequence.

ECHOCARDIOGRAPHY. High-frequency (40 MHz) transthoracic echocardiography was performed at each post-MI study interval in DKO mice to evaluate any differences in left ventricular (LV) diameter, infarct size, stroke volume, or peak aortic shear rate

FIGURE 3 Effect of ADAMTS13 Therapy and Platelet Depletion on Remote Arterial Activation

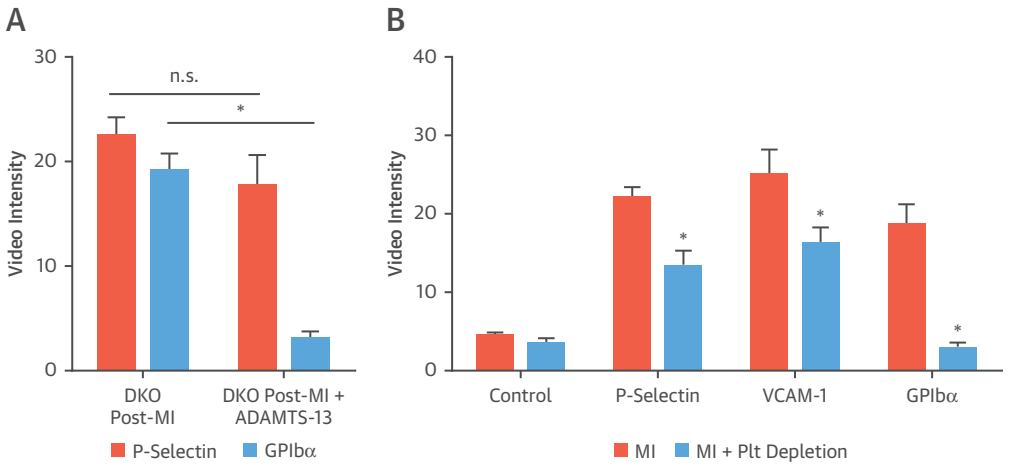

(A) CEU molecular imaging intensity for P-selectin and platelet GPIbα in DKO mice at day 3 post-MI before and 1 h after ADAMTS-13 (5 μg, intravenously). **(B)** Aortic molecular imaging signal in DKO mice with and without platelet (Plt) depletion at 21 days post-MI. *$p < 0.05$ versus nontreated. ADAMTS13 = A disintegrin and metalloprotease with thrombospondin type I repeats-13; other abbreviations as in Figure 2.

related to treatment with apocynin. Parasternal long- and short-axis imaging planes at the mid-ventricular level were used to assess infarct size quantified by calculating a wall motion score index. LV dimensions at end-systole and -diastole were measured from the parasternal long-axis view using linear measurements of the LV at the level of the mitral leaflet tips during diastole. Stroke volume was calculated as the product of the LV outflow tract cross-sectional area and time-velocity integral on pulsed-wave Doppler. Longitudinal strain was calculated using speckle-tracking echocardiography from a parasternal long-axis view and was quantified as the average of a standard single 6-segment model.

HISTOLOGY. Histology of the aortic root and the mid-ascending aorta for DKO mice was performed 21 days or 3 months after MI (randomized evenly for each group). Perfusion-fixed transaxial sections were stained with Masson's trichrome for assessment of plaque area and collagen content. Immunohistochemistry was performed with antibody against Mac-2 (M3/38, Thermofisher Science, Waltham, Massachusetts) to assess macrophage content, against CD41 (sc20234, Santa Cruz Biotechnology, Santa Cruz California) for platelets, and for VCAM-1 (BS-0369r, Bioss Inc., Atlanta, Georgia). For each epitope, secondary staining was performed with species-appropriate secondary antibodies labeled with ALEXAFluor-488, -555, or -594 (Invitrogen, Grand Island, New York). Plaque collagen content, necrotic core, and MAC-2 area are expressed as percent of plaque area.

INTRAVITAL MICROSCOPY. Direct observation of post-MI potentiation of platelet- and leukocyte-endothelial interactions was performed with intravital microscopy in wild-type and DKO mice, with or without MI, 3 days prior to study. Mice were anesthetized with ketamine and xylazine (intraperitoneally), and the cremaster muscle was exteriorized and prepared for intravital microscopy as previously described (16). Microscopy was performed with combined fluorescent epi-illumination and low-intensity transillumination (Axioskop2-FS, Carl Zeiss, Inc., Thornwood, New York) and digital recordings were made with a high-resolution CCD camera (C2400, Hamamatsu Photonics, Hamamatsu City, Japan). In vivo fluorescent labeling of platelets was performed with rhodamine-6G (1 mg/ml, 75 μl IV). The number of adherent leukocytes and platelet adhesive events (>5 s), and the formation of platelet "strings" indicative of ultralarge VWF multimers were quantified as fluorescent platelet area normalized to vessel area. Rolling velocity of leukocytes in 15- to 35-μm post-capillary venules was calculated by the distance traveled by video calipers divided by time.

STATISTICAL ANALYSIS. Data analysis was performed with Prism version 7.0a (Graph Pad, La Jolla, California). Continuous variables that were normally distributed are displayed as mean ± SD unless stated

FIGURE 4 Effect of Apocynin on Remote Endothelial Activation

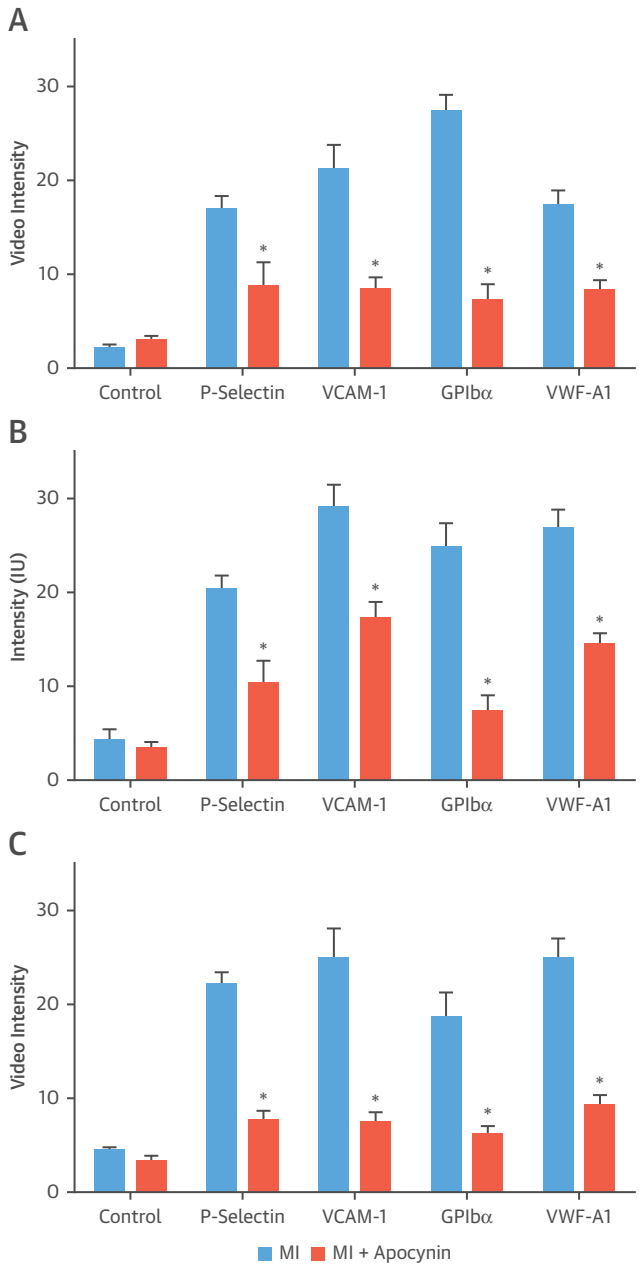

Mean ± SEM signal intensity on quantitative CEU molecular imaging depicting effect of apocynin in: **(A)** wild-type mice 3 days post-MI; **(B)** DKO mice 3 days post-MI; and **(C)** DKO mice 21 days post-MI. *p < 0.05 versus nontreated. Abbreviations as in Figure 2.

otherwise, whereas those that were not normally distributed are displayed as box-whisker plots with a bar representing median, box representing 25% to 75% quartiles, and whiskers representing range. Student's *t*-tests (paired or unpaired) were performed for comparisons of normally distributed data. For non-normally distributed data, either a Mann-Whitney *U* test or Wilcoxon signed rank test was used as appropriate according to experimental conditions (group-wise comparisons versus paired data within a group). For multiple comparisons, a 1-way analysis of variance was performed for normally distributed data with post-hoc testing with Holm-Sidak's multiple comparisons correction. A Kruskal-Wallis test followed by Dunn's multiple comparison test was performed for non-normally distributed data.

RESULTS

POST-MI VENTRICULAR FUNCTION AND AORTIC SHEAR. Electrocardiographic ST-segment elevation and regional hypokinesis or akinesis involving the mid to distal anterior, anterolateral, and anteroseptal walls on echocardiography was observed in all mice at the time of closed-chest left anterior descending coronary artery ischemia, but were not seen in any of the animals undergoing sham surgical procedure. MI resulted in LV enlargement, reduction of LV systolic function and stroke volume at days 3 and 21 (Figure 1). Chronic therapy with apocynin starting on the day of MI did not affect the infarct-related changes in LV dimension or function on echocardiography.

REMOTE ARTERIAL ENDOTHELIAL ACTIVATION AND PLATELET ADHESION AFTER MI. At baseline prior to any procedures, molecular imaging signal enhancement of the thoracic aorta for endothelial P-selectin, VCAM-1, VWF A1-domain, and platelet GPIbα were all found to be higher in DKO than wild-type mice (Figure 2A), consistent with greater aortic endothelial adhesion molecule expression, endothelial-associated active form of VWF, and platelet adhesion in DKO mice. In DKO but not wild-type mice, signal for all 4 targeted microbubble agents was significantly greater than for control microbubbles. At day 3 post-MI, signal for endothelial P-selectin, VCAM-1, VWF, and platelet GPIbα all increased significantly in both wild-type and DKO mice (Figures 2B to 2D). In wild-type mice, the post-MI increase for all 4 targeted agents completely resolved and returned to baseline levels at day 21, whereas in DKO mice, signal enhancement remained elevated at 21 days. Signal from control MBs was low in all mice and did not change significantly after MI. Sham procedure did not produce any changes on CEU molecular imaging (Figure 2E).

EFFECT OF ADAMTS13 ON PLATELET ADHESION. In DKO mice, aortic CEU molecular imaging 3 days post-MI was performed before and 1 h after treatment with recombinant ADAMTS13, a protease that

FIGURE 5 Remote Microvascular Endothelial Activation

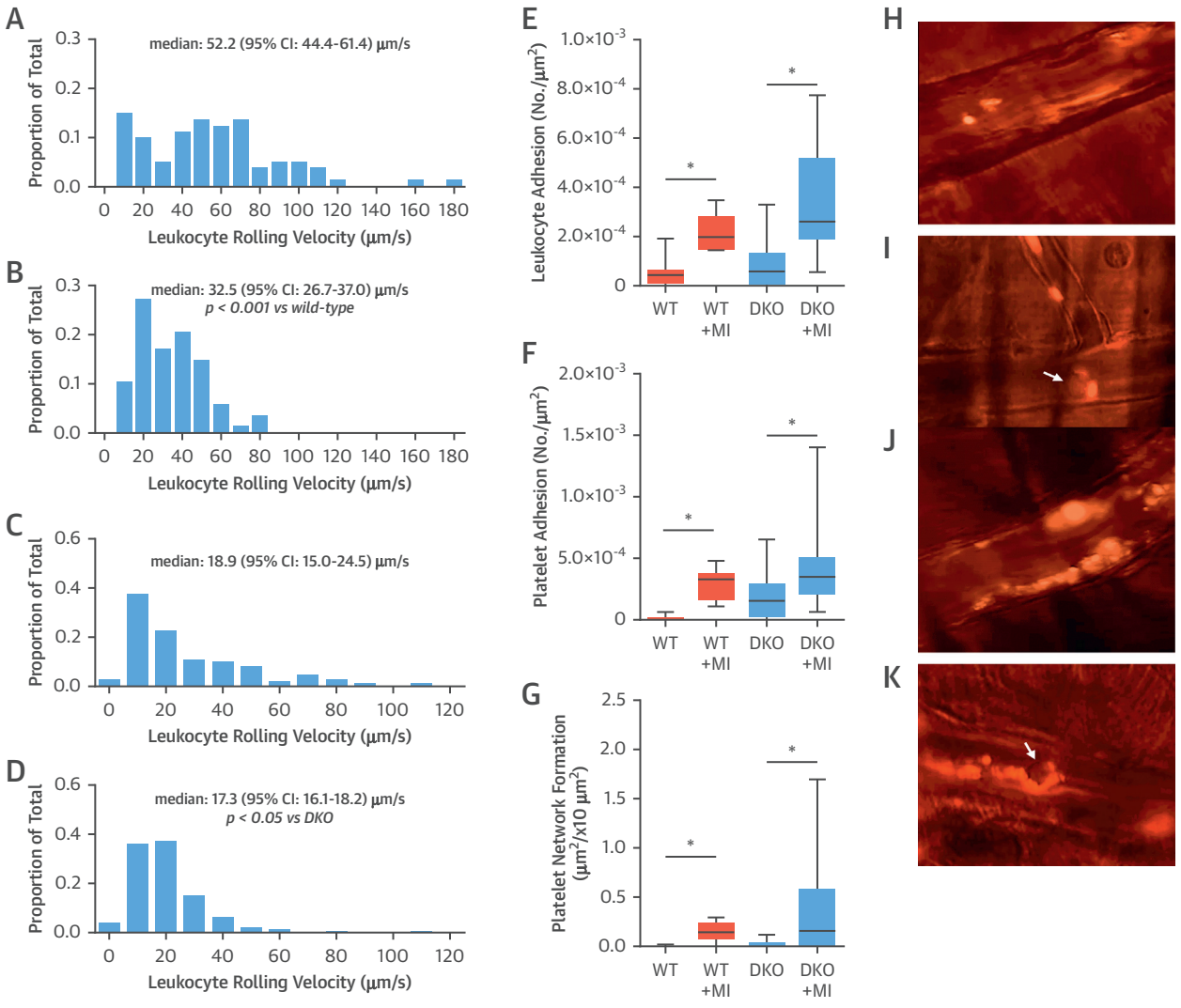

Histograms and median leukocyte rolling velocities in cremasteric venules are shown for **(A)** wild-type (WT) mice, **(B)** WT mice 3 days post-MI, **(C)** DKO mice, and **(D)** DKO mice 3 days post-MI. Box-whisker plots depict **(E)** leukocyte adhesion (number per vessel area); **(F)** isolated platelet adhesion; and **(G)** platelet string or net complex formation rate on venules. *p < 0.001; †p < 0.0001. Pseudocolorized intravital microscopy images illustrate rhodamine-6G-labeled platelets adhering in post-capillary venules in the form of: **(H)** individual platelets; **(I)** single platelet-leukocyte complex; **(J)** large platelet net complexes on the endothelium; and **(K)** platelet strings attached (downstream) to adherent leukocytes. Online Videos 1, 2, 3 and 4 illustrate different forms of platelet-endothelial interaction. **Arrows** indicate leukocytes. CI = confidence interval; other abbreviations as in Figure 2.

removes endothelial-associated VWF and regulates VWF multimer size (10,17). ADAMTS13 abolished platelet GPIbα signal (Figure 3A), indicating that platelet adhesion in remote vessels after MI occurs secondary to inducible abnormalities in the enzymatic regulation of endothelial-associated VWF. The lack of effect on P-selectin signal confirmed that this signal was primarily endothelial rather than platelet in origin.

EFFECT OF PLATELET DEPLETION ON ENDOTHELIAL ACTIVATION. In DKO mice studied at day 21, platelet immune-depletion started on day 1 after MI completely prevented the post-MI increase in platelet adhesion on aortic molecular imaging, and also significantly but modestly reduced endothelial P-selectin and VCAM-1 signal enhancement (Figure 3B).

NOX INHIBITION REDUCES ENDOTHELIAL ACTIVATION AND PLATELET ADHESION. Apocynin started on the

FIGURE 6 Aortic Histology From DKO Mice

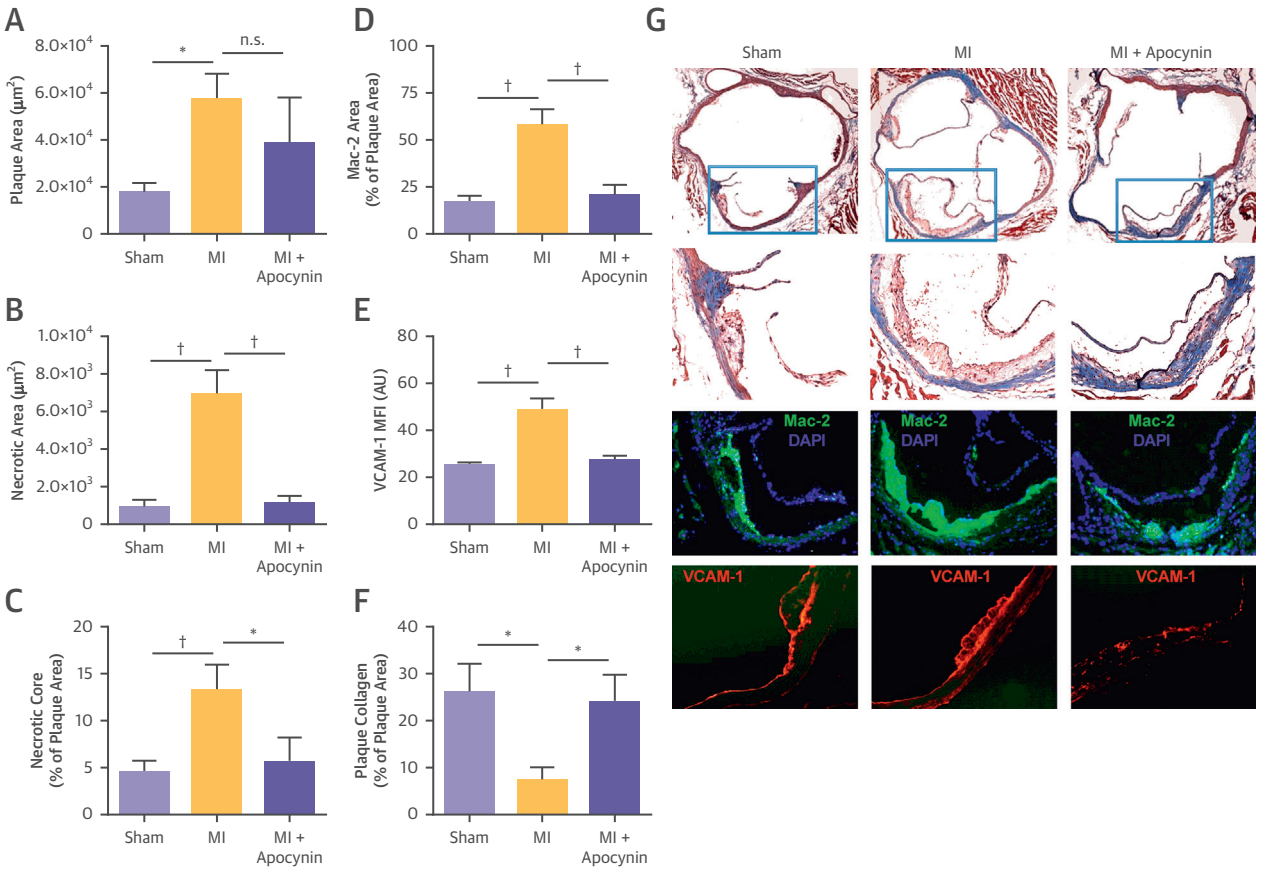

Data are from DKO mice at 21 days after sham procedure or after MI, with or without apocynin treatment. **(A)** Plaque cross-sectional area averaged for the aortic sinuses and distal ascending aorta; **(B)** necrotic core area; **(C)** necrotic core area as a percentage of total plaque area; **(D)** Mac-2 area averaged for plaques in the aortic sinuses and distal ascending aorta; **(E)** VCAM-1 staining area; and **(F)** plaque collagen content as a percentage of the total plaque area. *p < 0.05; †p < 0.01. **(G)** Examples of histology with Masson's trichrome, and immunohistochemistry for Mac-2 and VCAM-1 from DKO mice 21 days after either sham procedure or MI with or without apocynin treatment. Higher resolution images from day-21 and 3-month data are provided in Online Figures 1 and 2.

day of MI significantly attenuated the post-MI increase in remote aortic molecular imaging signal for P-selectin, VCAM-1, platelet GPIbα, and VWF A-1 in wild-type mice at day 3 and in DKO mice at days 3 and 21 (**Figures 4A to 4C**).

REMOTE ENDOTHELIAL ACTIVATION IN THE MICROCIRCULATION. Intravital microscopy of the cremaster muscle was used to interrogate for similar post-MI remote endothelial-related events in the microcirculation. Venular leukocyte rolling velocity in both wild-type and DKO mice decreased after MI (**Figures 5A to 5D**, Online Videos 1, 2, 3 and 4). Leukocyte firm adhesion in venules and platelet adhesion were also significantly increased 3 days post-MI in both wild-type and DKO mice (**Figures 5E to 5G**). Almost all platelet adhesion events in nonischemic mice were in the form of single platelets or small linear aggregates, whereas platelet adhesion post-MI was in the form of large string or net assemblies, consistent with ultralarge multimers of VWF on the endothelium or anchored to adherent leukocyte-platelet hetero-aggregates (**Figures 5H to 5K**, Online Videos 1, 2, 3 and 4).

POST-MI ACCELERATION OF PLAQUE PROGRESSION IS SUPPRESSED WITH NOX-2 INHIBITION. Aortic histology demonstrated that at 21 days, DKO mice undergoing MI compared with sham-treated mice had larger plaque area, larger necrotic core area, increased macrophage content, greater VCAM-1 staining, and lower collagen content (**Figure 6,** Online Figure 1).

CENTRAL ILLUSTRATION **Remote Endothelial Activation After Myocardial Infarction**

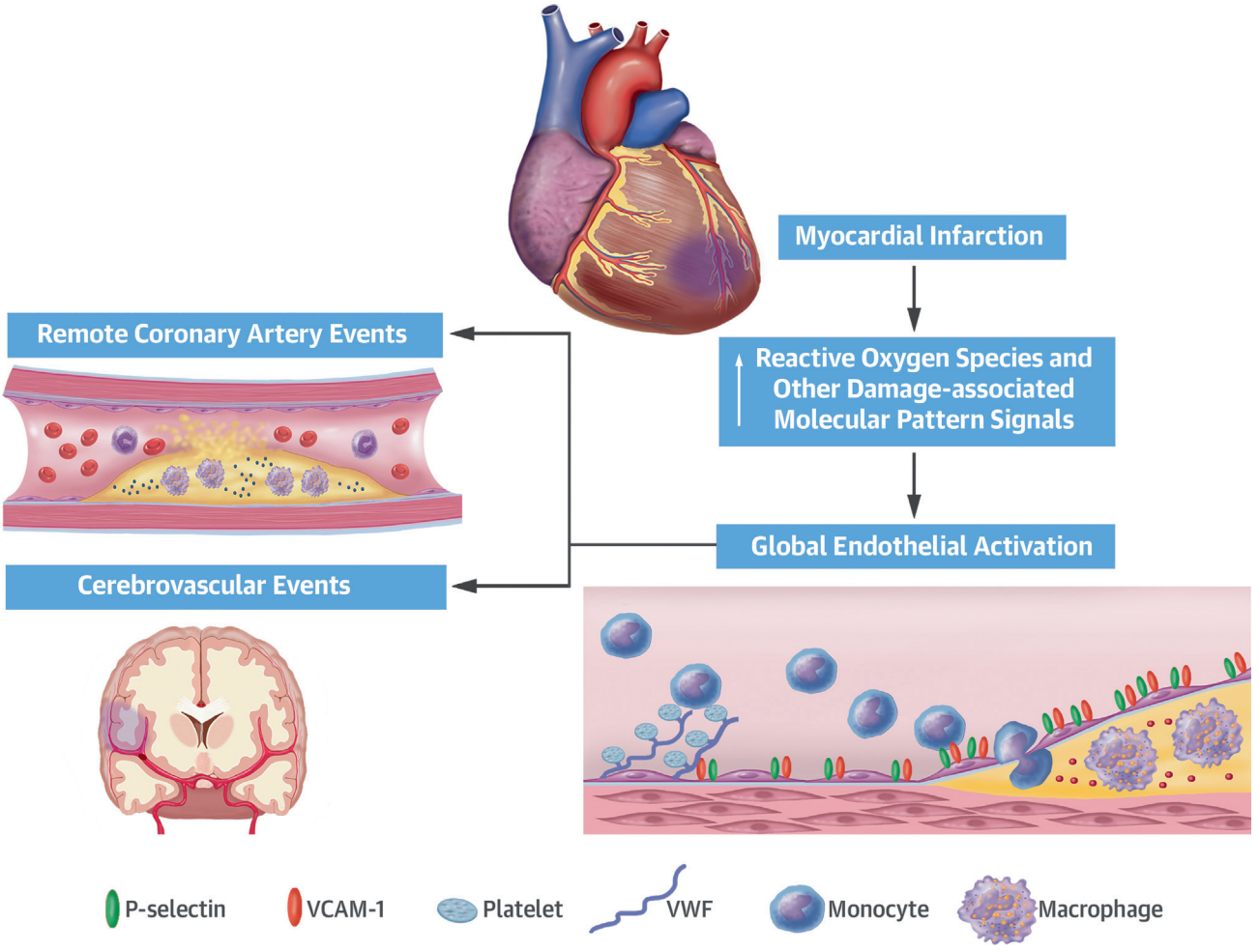

Moccetti, F. et al. J Am Coll Cardiol. 2018;72(9):1015–26.

Myocardial infarction triggers systemic effects, including an increase in reactive oxygen species and other damage-associated molecular patterns. These molecular intermediates result in endothelial activation, including up-regulation of adhesion molecules for inflammatory cells, increase in endothelial associated von Willebrand factor (VWF), and secondary platelet adhesion. The proinflammatory and prothrombotic endothelial changes found in our experiments could be associated with increased risk for atherothrombotic events in humans. VCAM = vascular cell adhesion molecule.

The increase in VCAM-1 staining was present in endothelium overlying atherosclerotic plaques, as well as nonplaque endothelium. Apocynin therapy in post-MI DKO mice attenuated all of the high-risk features in terms of macrophage content, VCAM-1 staining, and collagen content, whereas the reduction in plaque size did not reach statistical significance. Histology obtained at 3 months demonstrated persistently larger plaque size and macrophage content and lower collagen content in DKO mice undergoing MI compared with sham-treated control mice (Online Figure 2).

DISCUSSION

Our results indicate that acute MI stimulates a spectrum of adverse events in remote arterial and microvascular beds including endothelial up-regulation of VCAM-1 and P-selectin, and platelet adhesion that occurs through primarily through VWF that is either endothelial-associated or from adherent leukocyte-platelet complexes (**Central Illustration**). These adverse changes at the vascular endothelial surface persist longer when there is pre-existing atherosclerosis and hyperlipidemia, and are associated with

acceleration of plaque growth and inflammation in arteries spatially remote from the MI. Our data also suggest that reduction of oxidative stress through Nox inhibition attenuates adverse endothelial responses in remote arteries.

There is increasing evidence that global inflammatory responses after a major acute ischemic event contribute to the heightened risk for events in remote arterial beds. Leukocytosis and elevated plasma levels of cytokines and chemokines commonly occurs in the subacute phase after MI, the degree of which is associated with intermediate-term prognosis (18–20). In studies performed in atherosclerotic mice, acute MI has been shown to lead to an increase of proinflammatory Ly-6C^{high} monocytes and other myeloid cells (4). Carotid activity with 18F-fluorodeoxyglucose positron emission tomography has been shown to be higher in patients with recent acute MI than those with chronic stable angina (21), although cross-sectional design precluded any comments on causation. Little is known regarding endothelial changes that promote the recruitment of innate immune cells into atherosclerotic lesions in distant vessels after MI.

We applied CEU molecular imaging with targeted tracers confined to the vascular compartment to reveal that reperfused MI triggers remote arterial up-regulation of endothelial cell adhesion molecules that are critical for the recruitment of inflammatory cells (9,22). Although our primary aim was to study events in large arteries, corroborative evidence in other vascular territories was provided by intravital microscopy of a noncoronary microvascular bed, where leukocyte rolling velocity and adhesion were used as indicators of endothelial expression of selectins and integrin counter-receptors. These studies confirmed that MI promotes global endothelial activation. We believe that endothelial activation was in part responsible for the acceleration of plaque growth, inflammation, and necrotic core at 21 days and 3 months post-MI; these effects are consistent with a more "high risk" plaque appearance on histology. However, it is possible that increased plaque macrophage content contributed to the persistence of the endothelial activation at day 21 in DKO mice, consistent with the feed-forward nature of plaque inflammation.

Our investigation of endothelial-platelet adhesion after MI is based on the mounting evidence that these interactions play a multifactorial role in promoting plaque inflammation (9,23). Local release of platelet-derived proinflammatory cytokines and CD40L leads to monocyte activation, up-regulation of endothelial adhesion molecules, formation of neutrophil extracellular traps, and the generation of reactive oxygen species (ROS) (9,23–25). Inhibition of platelet activation or adhesion has been shown in animal models to reduce plaque size and inflammation (26,27).

Platelet adhesion in early- to moderate-stage atherosclerosis is primarily mediated by interactions between the GPIbα component of the GPIb/IX/V complex on platelets and the A1 domain of "activated" VWF (27–29). This interaction appears to be facilitated by association of VWF with the intact endothelial surface and ineffective cleavage at the A2 domain by ADAMTS13, resulting in ultra-large multimers of self-associated VWF (17,29,30). In this study, molecular imaging of a remote artery revealed a large increase in endothelial VWF-A1 domain and platelet adhesion after MI, which paralleled endothelial inflammatory responses. Platelet signal in post-MI DKO mice was entirely eliminated by exogenous ADAMTS13 implicating abnormal regulation of VWF. Again, intravital microscopy provided corroborative evidence, such as the formation of large linear platelet clusters that were dynamic in size and oscillated in flow, characteristic of the large VWF networks. To a lesser degree, adherent platelet-monocyte complexes were also observed. Many of these hetero-aggregates did not appear consistent with direct contact of single platelets to the leukocyte surface, but instead appeared as a dynamic clustering of platelets downstream from leukocytes possibly consistent with VWF net formation on leukocytes (31). The contribution of platelets to post-MI endothelial activation in this study was confirmed by a reduction, but not elimination, of P-selectin and VCAM-1 signal at 21 days in platelet-depleted DKO mice.

Oxidative stress measured by a variety of biomarkers is known to increase after recent MI (32), is known to be greater in the setting of dyslipidemia (33), and represents a pathway by which inflammation and platelet adhesion can self-propagate in a deleterious manner (9). We evaluated the contribution of oxidative stress by treating mice with apocynin, which, among many of its effects, inhibits membrane translocation of the p47*phox* and gp91*phox* subunits of Nox (13), and in our experience, has been more effective at reducing adhesion molecule expression than free radical scavenger approaches. Apocynin was found to reduce molecular imaging signal for P-selectin, VCAM-1, VWF-A1, and platelet GPIbα. These data suggest that increased oxidative stress plays an important role in remote endothelial activation after MI. These findings are consistent with known effects of reactive oxygen species to stimulate

adhesion molecule expression through the transcription factor nuclear factor-κB and to inhibit proteolytic regulation of VWF (34–36). The suppression of adhesion molecule expression and platelet adhesion with apocynin was associated with partial protection from post-MI accelerated plaque progression in terms of inflammation and necrotic core size.

STUDY LIMITATIONS. Although the murine model was selected to reflect human disease based on reproducible plaque development without extreme diet, mice do not necessarily reproduce human condition based on both plaque location and lack of plaque rupture or erosion as the inciting event. It is also important to note that post-MI molecular imaging and plaque assessment were made only for the aorta based on the inability to resolve smaller branch nonculprit arteries and because of the unique distribution of disease in murine models. We did not make any direct measurements of oxidative stress in the different cohorts, largely because of the strength of evidence from previous studies demonstrating that oxidative biomarkers increase after MI and are reduced by apocynin (32,37). There are insufficient data to state that the primary mechanism by which apocynin reduced plaque progression after MI was directly attributable to adhesion molecule expression and platelet adhesion. Instead, we believe that lowering ROS would have pleiotropic effects that would include the endothelial abnormalities that were the focus of this study. Importantly, we do not yet have data revealing the primary inciting factor for remote plaque activation, nor do we have data on how infarct size or duration of ischemia influence the degree of remote plaque activation.

CONCLUSIONS

MI leads to remote endothelial activation and abnormal regulation of endothelial-associated and possibly leukocyte-associated VWF (**Central Illustration**). These processes are associated with enhanced monocyte recruitment, platelet-endothelial adhesion, and acceleration of plaque progression. Interrupting the endogenous vascular production of ROS with the Nox inhibitor apocynin suppresses adverse remote endothelial changes. Our findings help clarify the mechanisms for heightened risk for recurrent events after MI, and reveal potentially modifiable processes. They could also contribute to the mechanistic understanding of the recently described beneficial effects of proinflammatory cytokine inhibition in patients with MI (38).

ADDRESS FOR CORRESPONDENCE: Dr. Jonathan R. Lindner, Knight Cardiovascular Institute, UHN-62, Oregon Health & Science University, 3181 SW Sam Jackson Park Road, Portland, Oregon 97239. E-mail: lindnerj@ohsu.edu. Twitter: @OHSUSOM.

PERSPECTIVES

COMPETENCY IN MEDICAL KNOWLEDGE: Acute atherothrombotic events, such as MI and stroke, increase the risk of ischemic events in nonculprit arteries and other vascular territories for several months. These secondary events are mediated by up-regulation of endothelial inflammatory adhesion molecules and platelet-endothelium interactions that are associated with accelerated plaque inflammation and persist longer in the presence of hyperlipidemia.

TRANSLATIONAL OUTLOOK: Future research should examine inhibition of systemic inflammatory processes that promote endothelial adhesiveness and platelet-endothelium interactions to reduce recurrent ischemic events after MI.

REFERENCES

1. Stone GW, Maehara A, Lansky AJ, et al. A prospective natural-history study of coronary atherosclerosis. N Engl J Med 2011;364:226–35.

2. Witt BJ, Brown RD Jr., Jacobsen SJ, Weston SA, Yawn BP, Roger VL. A community-based study of stroke incidence after myocardial infarction. Ann Intern Med 2005;143:785–92.

3. Milonas C, Jernberg T, Lindback J, et al. Effect of angiotensin-converting enzyme inhibition on one-year mortality and frequency of repeat acute myocardial infarction in patients with acute myocardial infarction. Am J Cardiol 2010;105:1229–34.

4. Dutta P, Courties G, Wei Y, et al. Myocardial infarction accelerates atherosclerosis. Nature 2012;487:325–9.

5. Lee WW, Marinelli B, van der Laan AM, et al. PET/MRI of inflammation in myocardial infarction. J Am Coll Cardiol 2012;59:153–63.

6. Kaufmann BA, Carr CL, Belcik JT, et al. Molecular imaging of the initial inflammatory response in atherosclerosis: implications for early detection of disease. Arterioscler Thromb Vasc Biol 2010;30:54–9.

7. Shim CY, Liu YN, Atkinson T, et al. Molecular imaging of platelet-endothelial interactions and endothelial von Willebrand factor in early and mid-stage atherosclerosis. Circ Cardiovasc Imaging 2015;8:e002765.

8. Chadderdon SM, Belcik JT, Bader L, et al. Proinflammatory endothelial activation detected by molecular imaging in obese nonhuman primates coincides with onset of insulin resistance and progressively increases with duration of insulin resistance. Circulation 2014;129:471–8.

9. Wu MD, Atkinson TM, Lindner JR. Platelets and von Willebrand factor in atherogenesis. Blood 2017;129:1415–9.

10. Dong JF. Cleavage of ultra-large von Willebrand factor by ADAMTS-13 under flow conditions. J Thromb Haemost 2005;3:1710–6.

11. Ruggeri ZM. Von Willebrand factor, platelets and endothelial cell interactions. J Thromb Haemost 2003;1:1335–42.

12. Powell-Braxton L, Veniant M, Latvala RD, et al. A mouse model of human familial hypercholesterolemia: markedly elevated low density lipoprotein cholesterol levels and severe atherosclerosis on a low-fat chow diet. Nat Med 1998;4:934–8.

13. Yu J, Weiwer M, Linhardt RJ, Dordick JS. The role of the methoxyphenol apocynin, a vascular NADPH oxidase inhibitor, as a chemopreventative agent in the potential treatment of cardiovascular diseases. Curr Vasc Pharmacol 2008;6:204–17.

14. Impellizzeri D, Esposito E, Mazzon E, et al. Effect of apocynin, a NADPH oxidase inhibitor, on acute lung inflammation. Biochem Pharmacol 2011;81:636–48.

15. Kaufmann BA, Sanders JM, Davis C, et al. Molecular imaging of inflammation in atherosclerosis with targeted ultrasound detection of vascular cell adhesion molecule-1. Circulation 2007;116:276–84.

16. Lindner JR, Coggins MP, Kaul S, Klibanov AL, Brandenburger GH, Ley K. Microbubble persistence in the microcirculation during ischemia/reperfusion and inflammation is caused by integrin- and complement-mediated adherence to activated leukocytes. Circulation 2000;101:668–75.

17. Dong JF, Moake JL, Nolasco L, et al. ADAMTS-13 rapidly cleaves newly secreted ultralarge von Willebrand factor multimers on the endothelial surface under flowing conditions. Blood 2002;100:4033–9.

18. Madjid M, Awan I, Willerson JT, Casscells SW. Leukocyte count and coronary heart disease: implications for risk assessment. J Am Coll Cardiol 2004;44:1945–56.

19. Fang L, Moore XL, Dart AM, Wang LM. Systemic inflammatory response following acute myocardial infarction. J Geriatr Cardiol 2015;12:305–12.

20. Gonzalez-Quesada C, Frangogiannis NG. Monocyte chemoattractant protein-1/CCL2 as a biomarker in acute coronary syndromes. Curr Atheroscler Rep 2009;11:131–8.

21. Kim EJ, Kim S, Kang DO, Seo HS. Metabolic activity of the spleen and bone marrow in patients with acute myocardial infarction evaluated by 18f-fluorodeoxyglucose positron emission tomographic imaging. Circ Cardiovasc Imaging 2014;7:454–60.

22. Galkina E, Ley K. Vascular adhesion molecules in atherosclerosis. Arterioscler Thromb Vasc Biol 2007;27:2292–301.

23. Nording HM, Seizer P, Langer HF. Platelets in inflammation and atherogenesis. Front Immunol 2015;6:98.

24. Langer HF, Gawaz M. Platelet-vessel wall interactions in atherosclerotic disease. Thromb Haemost 2008;99:480–6.

25. Henn V, Slupsky JR, Grafe M, et al. CD40 ligand on activated platelets triggers an inflammatory reaction of endothelial cells. Nature 1998;391:591–4.

26. Huo Y, Schober A, Forlow SB, et al. Circulating activated platelets exacerbate atherosclerosis in mice deficient in apolipoprotein E. Nat Med 2003;9:61–7.

27. Massberg S, Brand K, Gruner S, et al. A critical role of platelet adhesion in the initiation of atherosclerotic lesion formation. J Exp Med 2002;196:887–96.

28. Theilmeier G, Michiels C, Spaepen E, et al. Endothelial von Willebrand factor recruits platelets to atherosclerosis-prone sites in response to hypercholesterolemia. Blood 2002;99:4486–93.

29. Liu Y, Davidson BP, Yue Q, et al. Molecular imaging of inflammation and platelet adhesion in advanced atherosclerosis effects of antioxidant therapy with NADPH oxidase inhibition. Circ Cardiovasc Imaging 2013;6:74–82.

30. Chauhan AK, Goerge T, Schneider SW, Wagner DD. Formation of platelet strings and microthrombi in the presence of ADAMTS-13 inhibitor does not require P-selectin or beta3 integrin. J Thromb Haemost 2007;5:583–9.

31. Pendu R, Terraube V, Christophe OD, et al. P-selectin glycoprotein ligand 1 and beta2-integrins cooperate in the adhesion of leukocytes to von Willebrand factor. Blood 2006;108:3746–52.

32. Neri M, Fineschi V, Di Paolo M, et al. Cardiac oxidative stress and inflammatory cytokines response after myocardial infarction. Curr Vasc Pharmacol 2015;13:26–36.

33. Araujo FB, Barbosa DS, Hsin CY, Maranhao RC, Abdalla DS. Evaluation of oxidative stress in patients with hyperlipidemia. Atherosclerosis 1995;117:61–71.

34. Kunsch C, Medford RM. Oxidative stress as a regulator of gene expression in the vasculature. Circ Res 1999;85:753–66.

35. Chen J, Fu X, Wang Y, et al. Oxidative modification of von Willebrand factor by neutrophil oxidants inhibits its cleavage by ADAMTS13. Blood 2010;115:706–12.

36. Drummond GR, Selemidis S, Griendling KK, Sobey CG. Combating oxidative stress in vascular disease: NADPH oxidases as therapeutic targets. Nat Rev Drug Discov 2011;10:453–71.

37. Li B, Tian J, Sun Y, et al. Activation of NADPH oxidase mediates increased endoplasmic reticulum stress and left ventricular remodeling after myocardial infarction in rabbits. Biochimica et biophysica acta 2015;1852:805–15.

38. Ridker PM, Everett BM, Thuren T, et al. Anti-inflammatory Therapy with Canakinumab for Atherosclerotic Disease. N Engl J Med 2017;377:1119–31.

KEY WORDS adhesion molecules, myocardial infarction, platelets, von Willebrand factor

APPENDIX For supplemental figures and videos, please see the online version of this paper.